Mon. Not. R. Astron. Soc. (2005) doi:10.1111/j.1745-3933.2005.00099.x

Morphology of the coronal-line region in active galactic nuclei⋆

M. Almudena Prieto,[1]† Olivier Marco[2] and Jack Gallimore[3]
[1]*Max-Planck-Institut für Astronomie, Königstuhl 17, D-69117 Heidelberg, Germany*
[2]*ESO Paranal, Alonso de Cordova 3107, Vitacura, Santiago, Chile*
[3]*Department of Physics, Bucknell University, Lewisburg, PA 17837, USA*

Accepted 2005 August 26. Received 2005 August 22; in original form 2005 June 16

ABSTRACT

We present new images of the coronal-line region, as traced by [Si VII] 2.48 μm, in some of the nearest Seyfert 2 galaxies. In each of these galaxies, the coronal-line emission comprises a bright, compact central source and extended emission showing broad alignment along a particular direction, usually coinciding with that defined by the radio emission or the extended narrow-line region. The full extent of the coronal-line emission ranges from a few tens of parsecs to ∼150 pc radius from the nucleus and is a factor of ∼10 smaller than that seen in the extended, lower ionization gas. With a spatial resolution of 10 pc or better, the coronal region shows diffuse and filamentary structure in all cases, and it is difficult to see whether it breaks down into discrete blobs such as those seen in lower ionization lines or radio images of comparable resolution. The extent of the coronal-line emission is larger than would be predicted by photoionization models, which argues for additional *in situ* gas excitation, the most plausible energy source being shock excitation.

Key words: galaxies: nuclei – galaxies: Seyfert – infrared: galaxies.

1 INTRODUCTION

Coronal lines are collisionally excited forbidden transitions within low-lying levels of highly ionized species (ionization potential >100 eV). As such, these lines form in extreme energetic environments and thus are unique tracers of active galactic nucleus (AGN); they are not seen in starburst galaxies. Coronal lines appear from X-rays to infrared (IR) and are common in AGN regardless of their type (Penston et al. 1984; Marconi et al. 1994; Prieto & Viegas 2000). The strongest ones are seen in the IR; in the near-IR they can even dominate the line spectrum (Reunanen et al. 2003).

Owing to the high ionization potential, these lines are expected to be limited to a few tens to hundreds of parsecs around the active nucleus. Given those sizes, we started an adaptive optics assisted imaging programme with the European Southern Observatory/Very Large Telescope (ESO/VLT) aimed at revealing the detailed morphology of the CLR in some of nearest Seyfert galaxies. We use as a tracer the isolated IR line [Si VII] 2.48 μm (ionization potential = 205.08 eV). This Letter presents the resulting narrow-band images of the [Si VII] emission line, which reveal for the first time the detailed morphology of the CLR, and with suitable resolution for comparison with radio and optical lower ionization gas images. The morphology of the CLR is sampled with a spatial resolution almost a factor of 5 better than any previously obtained, corresponding to scales $\lesssim$10 pc. The galaxies presented are all Seyfert type 2: Circinus, NGC 1068, ESO 428-G1 and NGC 3081. Ideally, we would have liked to image type 1 objects, but, in the southern hemisphere, there are as yet no known suitable type 1 sources at sufficiently low redshift to guarantee the inclusion of [Si VII] 2.48 μm entirely in the filter passband.

2 OBSERVATIONS, IMAGE REGISTRATION AND ASTROMETRY

Observations were done with the adaptive optics assisted IR camera NACO at the ESO/VLT. Two narrow-band filters, one centred on the coronal [Si VII] 2.48-μm line and an adjacent band centred on 2.42-μm line-free continuum, were used. For each filter, the photometry was calibrated against standard stars observed after each science target. The wavefront sensor of the adaptive optics system followed the optical nucleus of the galaxies to determine seeing corrections.

The achieved spatial resolution was estimated from stars available in the field of the galaxies except in NGC 3081 and 1068 (cf. Table 1). The resolutions were comparable in both filters within the reported errors in Table 1. Continuum-free [Si VII] 2.48-μm line images are shown in Figs 1 and 2 for each galaxy. The total integrated coronal-line emission derived from these images is listed in Table 2. For comparison, [Si VII] 2.48-μm fluxes derived from long-slit spectroscopy are also provided.

Also in these figures, images with the 2.48-μm filter of the standard stars – also used as PSF control – are shown. The images provide a rough assessment of the image quality/resolution achieved in the science frames. For Circinus and ESO 428-G014, a more accurate evaluation is possible from field stars. One of these field stars

⋆Observations done under ESO/VLT programmes 70.B-0409 and 74.B-0404.

†E-mail: prieto@mpia.de

Table 1. Galaxy scales and achieved NACO angular resolution.

AGN	1 arcsec in pc	Stars in field	FWHM arcsec	FWHM pc	Nuc. size FWHM arcsec
Circinus	19	2	0.19±0.02	3.6	0.27
NGC 1068	70	0	0.097*	6.8	<0.097
ESO 428	158	3	0.084±0.006	13	0.15±0.01
NGC 3081	157	0	0.095*	14	<0.32

*In NGC 1068 the size of the nucleus is given as *K*-band interferometry sets an upper limit for the core of 5 mas (Weigelt et al. 2004); in NGC 3081, the size of a PSF star taken after the science frames is given.

is shown in both filters in Figs 1(e) and 2(b) respectively. To assess the image quality at the lowest signal levels, the images of the field stars are normalized to the galaxy peak at the corresponding filter. These are much fainter than the galaxy nucleus, thus the stellar peak is a mere ∼5 per cent of the galaxy peak.

Radio and *HST* images were used to establish an astrometric reference frame for the CLR. For NGC 1068 (Figs 1a, b and c), the registration of optical *HST* and adaptive optics IR images by Marco et al. (1997; accuracy ∼ 0.05 arcsec) was adopted. In the comparison it is assumed that the peak emission in Marco et al.'s *K*-band image coincides with that in the NACO 2.42-μm continuum image. The comparison with the MERLIN 5-GHz image of Gallimore et al. (2004) was done assuming that the nuclear radio source 'S1' and the peak emission in the NACO 2.42-μm image coincide.

In Circinus (Figs 1d, e and f), the registration of NACO and *HST*/Hα images was done on the basis of 3–4 stars available in all fields. That provides an accurate registration better than 1 pixel (see Prieto et al. 2004). No radio image of comparable resolution is available for this galaxy.

For ESO 428-G014 (Figs 2a, b and c), NACO images were registered on the basis of three available stars in the field. Further registration with a Very Large Array (VLA) 2-cm image (beam 0.2 arcsec: Falcke et al. 1998) was made on the assumption that the continuum peak at 2.42 μm coincides with that of the VLA core. We adopted the astrometry provided by Falcke et al. (uncertainty ∼0.3 arcsec) who performed the registration of the 2-cm and the *HST*/Hα images, and plotted the *HST*/Hα atop the NACO coronal-line image following that astrometry.

NGC 3081 (Figs 2d, e and f) has no stars in the field. In this case NACO 2.42- and 2.44-μm images, and an additional NACO deep *Ks*-band image, were registered using the fact that the NACO adaptive optics system always centres the images at the same position of the detector within 1 pixel (0.027 arcsec scale). The registration with an *HST*/Wide Field Planetary Camera 2 (WFPC2) image at 7910 Å employed, as a reference, the outer isophote of the *Ks*-band image which shows very similar morphology to that of the *HST* image. Further comparison with an *HST* PC2 Hα image relied on the astrometry by Ferruit et al. (2000). The registration with an *HST*/Faint Object Camera (FOC) image at 2100 Å (F210M) was based on the assumption that the UV nucleus and the continuum peak emission at 2.42 μm coincide. The radio images available for this galaxy have a beam resolution >0.5 arcsec (Nagar et al. 1999) and are therefore not used in this work.

3 THE SIZE AND MORPHOLOGY OF THE CLR

In the four galaxies, the CLR resolves into a bright nucleus and extended emission along a preferred position angle, which usually coincides with that of the extended lower ionization gas. The size of the CLR is a factor of 3 to 10 smaller than that of the extended narrow-line region (NLR). The maximum radius (Table 2) varies from 30 pc in Circinus to 70 pc in NGC 1068, to $\gtrsim$120 pc in NGC 3081 and ESO 428-G014. The emission in all cases is diffuse or filamentary, and it is difficult to determine whether it further breaks down into compact knots or blobs such as those found in Hα, [O III] 5007 Å or radio images even though the resolutions are comparable.

In Circinus, [Si VII] 2.48-μm emission extends across the nucleus and aligns with the orientation of its one-sided ionization cone, seen in Hα or in [O III] 5007 Å (Wilson et al. 2000). In these lines, the counter-cone is not seen, but in [Si VII], owing to the reduced extinction, extended diffuse emission is detected at that position (Fig. 1f; Prieto et al. 2004). This is further confirmed with VLT/ISAAC spectroscopy which shows both [Si VII] 2.48 μm and [Si VI] 1.96 μm extending up to 30-pc radius from the nucleus (Rodriguez-Ardila et al. 2004).

In ESO 428-G014, the coronal emission is remarkably aligned with the radio jet (Fig. 2c). The 2-cm emission is stronger in the north-west direction, and [Si VII] is stronger in that direction too. Hα emission is also collimated along the radio structure, but the emission spreads farther from the projected collimation axis and to a larger radius from the nucleus (Fig. 2b). Both Hα and the 2-cm emission resolve into several blobs but the coronal emission is more diffuse.

In NGC 3081, the coronal emission resolves into a compact nuclear region and a detached faint blob at ∼120 pc north of it. The *HST* [O III] 5007 and Hα images show rather collimated structure extending across the nucleus along the north–south direction over ∼300 pc radius (Ferruit et al. 2000). Besides the nucleus, the second brightest region in those lines coincides with the detached [Si VII] emission blob (Fig. 2d). At this same position, we also find UV emission in the *HST* image at 2100 Å.

NGC 1068 shows the strongest [Si VII] 2.48-μm emission among the four galaxies, a factor of 3 larger than in Circinus, and the only case where the nuclear emission shows detailed structure. At ∼7 pc radius from the radio core S1, [Si VII] emission divides into three bright blobs. The position of S1 falls in between. The southern blob looks like a concentric shell. The northern blob coincides with the [O III] peak emission at the vortex of the ionization cone; the other two blobs are not associated with a particular enhancement in [O III] or radio emission (Figs 1b and c). [Si VII] depression at the position of S1 may indicate a very high ionization level there: the region being filled with e.g. [Fe X], [Si IX]. Besides, lower surface brightness gas, extending up to at least 70-pc radius is seen. This diffuse region is confirmed by VLT/ISAAC spectra, which reveal [Si VI]1.96 μm and [Si VII] 2.48 μm extending up to comparable radii (Rodriguez-Ardila et al. 2004). This diffuse emission shows slight enhancement at both sides of the 5-GHz jet, but the signal-to-noise ratio is low.

4 DISCUSSION

ESO 438-G014 and NGC 3081 show the largest and best-collimated [Si VII] emission, up to 150-pc radius from the nucleus. To reach those distances by nuclear photoionization alone would require rather low electron densities or a very strong (collimated) radiation field. Density measurements in the CLR are scarce: Moorwood et al. (1996) estimate a density $n_e \sim 5000$ cm^{-3} in Circinus on the basis of [Ne V] 14.3 μm/24.3 μm; Erkens et al. (1997) derive $n_e < 10^7$ cm^{-3} in several Seyfert 1 galaxies, on the basis of several optical [Fe VII] ratios. This result may be uncertain because the optical [Fe VII] are weak and heavily blended. Taking $n_e \sim 10^4$ cm^{-3} as a reference value, it results in an ionization parameter $U \lesssim 10^{-3}$ at 150 pc from the nucleus, which is far too low to produce strong

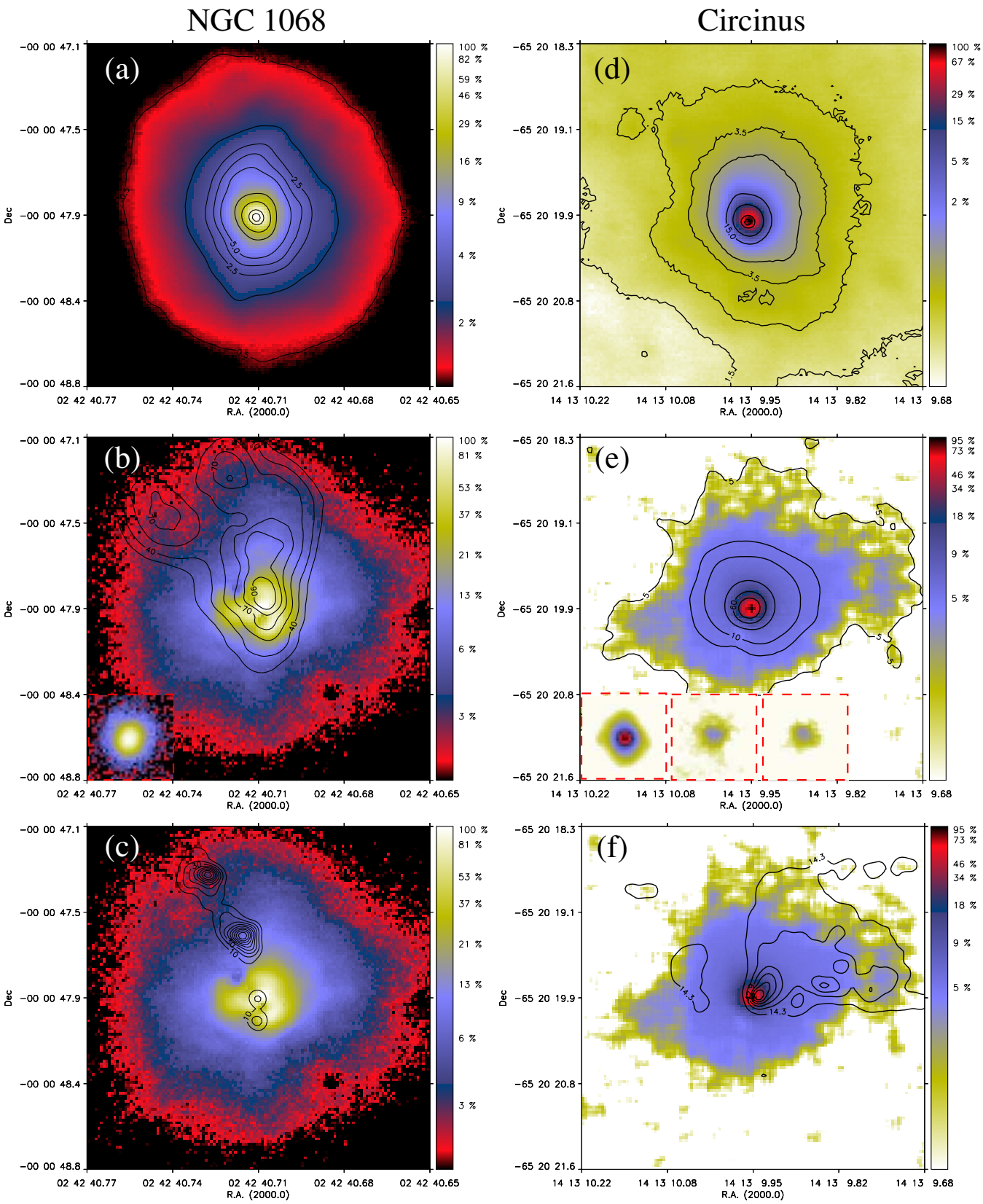

Figure 1. NACO images (log scale) overlaid with contours (unless indicated, numbers in contours and in the colour bar are in percentage of the maximum peak for both galaxies and stars). (a) 2.42-μm continuum. (b) [Si VII] 2.48 μm and *HST* [O III]5007 Å (contours). Inset: standard star in 2.48-μm filter. (c) [Si VII] 2.48 μm and MERLIN 5 GHz (Gallimore et al. 2004). (d) 2.42-μm continuum. (e) [Si VII] 2.48-μm line. Insets: left, standard star in 2.48-μm filter; centre and right: field star at 9.1 arcsec from nucleus and PA $= -30^{\circ}$, in 2.42- and 2.48-μm filters respectively, maximum normalized to the galaxy peak at that filter. (f) [Si VII] 2.48-μm and *HST* Hα (contours).

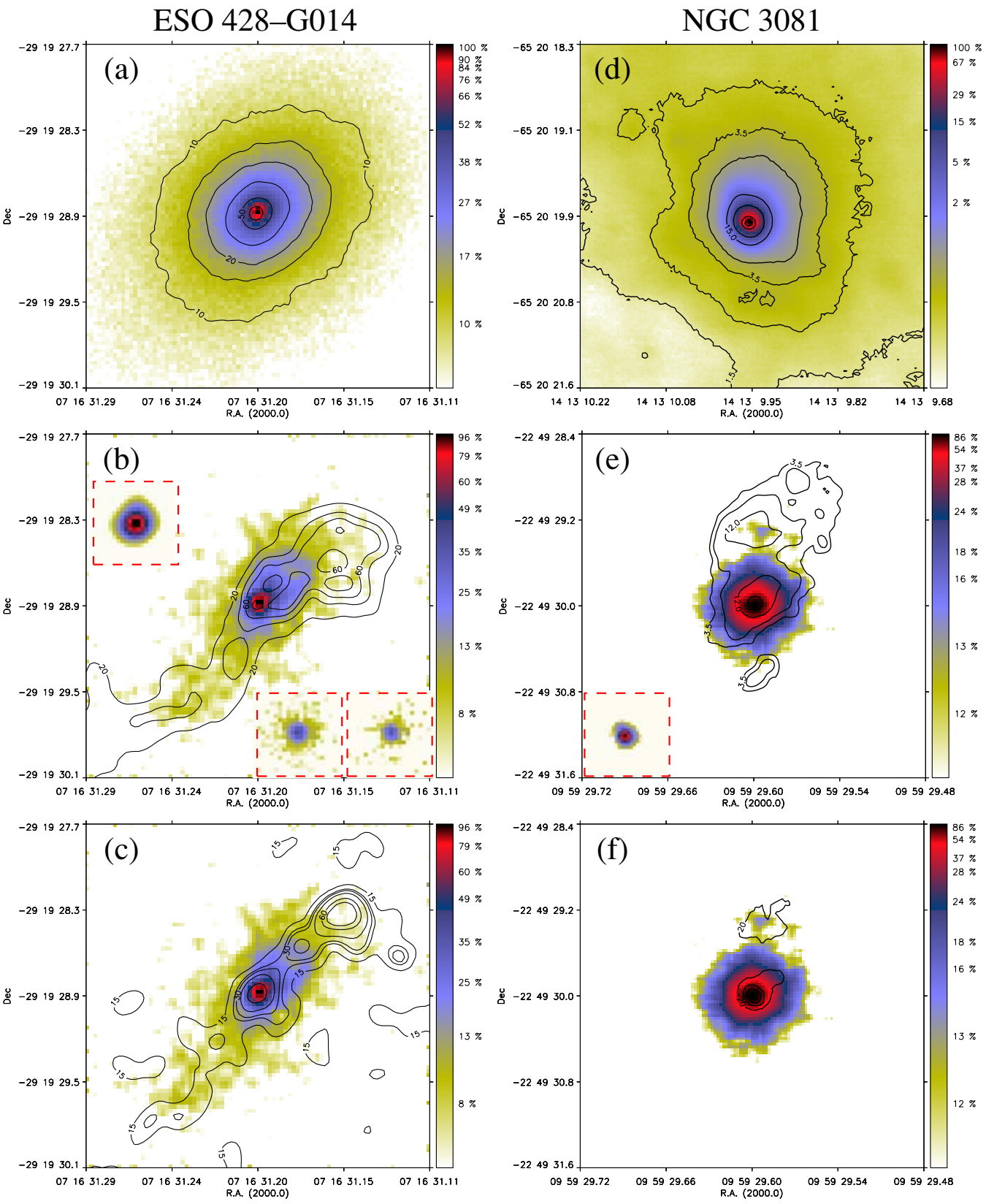

Figure 2. NACO images (colour code and contour numbers as in Fig. 1). (a) 2.42 μm continuum. (b) [Si VII] 2.48 μm and *HST* Hα (contours). Insets: top, standard star in 2.48-μm filter; bottom centre and right, field star at 11 arcsec from the nucleus and PA = 7°, in 2.42- and 2.48-μm filters respectively, normalized to the galaxy peak at that filter. (c) [Si VII] 2.48-μm and 2-cm VLA image (Falcke et al. 1998, contours). (d) 2.42-μm continuum. (e) [Si VII] 2.48-μm and *HST* Hα (contours). Inset: standard star in 2.48-μm filter. (f) [Si VII] 2.48-μm and *HST* UV 2100-Å (contours).

Table 2. Size and photometry of the 2.48 μm coronal-line region.

AGN	Radius from nucleus (pc)	Flux NACO in units of 10^{-14} erg s^{-1} cm^{-2}	Flux long-slit	Reference long-slit
Circinus	30	20	16	(1)
NGC 1068	70	72	47*	(2)
ESO 428-G014	120–160	2.0	0.7*	(2)
NGC 3081	120	0.8	0.8*	(2)

*In 1 × 1.4 arcsec^2 aperture. References: (1) Oliva et al. (1994); (2) Reunanen et al. (2003).

[Si VII] emission (see e.g. Ferguson et al. 1997; Rodriguez-Ardila et al., in preparation).

We argue that, in addition to photoionization, shocks must contribute to the coronal emission. This proposal is primarily motivated by a parallel spectroscopic study of the kinematics of the CLR gas (Rodriguez-Ardila et al., in preparation), which reveals coronal-line profiles with velocities $500 < v < 2000$ km s^{-1} . Here we assess the proposal in a qualitative manner, by looking for evidence for shocks from the morphology of the gas emission.

In ESO 428-G014, the remarkable alignment between [Si VII] and the radio emission is a strong indication of the interaction of the radio jet with the interstellar medium (ISM). There is spectroscopic evidence of a highly turbulent ISM in this object: asymmetric line profiles indicate gas velocities of up to 1400 km s^{-1} (Wilson & Baldwin 1989).

The concentric shell-like structure seen in NGC 3081 in [O III] 5007 Å and Hα (Ferruit et al. 2000) is even more suggestive of propagating shock fronts. From the [O III]/Hα map by Ferruit et al. the excitation level at the position of the [Si VII] northern blob is similar to that of the nucleus, which points to similar ionization parameter despite its distance from the nucleus. The cloud density might then decrease with distance to balance the ionization parameter, but this would demand a strong radiation field to keep line emission efficient. Alternatively, a local source of excitation is needed. The presence of co-spatial UV continuum, possibly locally generated bremsstrahlung, and [Si VII] line emission circumstantially supports the shock excitation proposal.

In the case of Circinus and NGC 1068, the morphological evidence for shocks from the [Si VII] images is less obvious. However, both galaxies present high-velocity nuclear outflows, which are inferred from the asymmetric and blueshifted profiles measured in the [O III] 5007 gas in the case of Circinus (Veilleux & Bland-Hawthorn 1997), and in the Fe and Si coronal lines in both. In the latter, velocities of ∼500 km s^{-1} in Circinus and ∼2000 km s^{-1} in NGC 1068 are inferred from the coronal profiles (Rodriguez-Ardila et al. 2004, also in preparation).

An immediate prediction for the presence of shocks is the production of free–free emission, with a maximum in the UV to X-ray, from the shock-heated gas. We make here a first-order assessment of this contribution using results from photoionization–shocks composite models by Contini et al. (2004), and compare it with the observed soft X-rays. For each galaxy, we derive the 1-keV emission due to free–free from models computed for a nuclear ionizing flux $F_{\rm h} = 10^{13}$ photon cm^{-2} s^{-1} eV^{-1}, pre-shock density $n_0 = 300$ cm^{-3} and shock velocity closer to the gas velocities measured in these galaxies (we use fig. A3 in Contini et al.). The choice of $F_{\rm h}$ has a low impact on the 1-keV estimate as the bremsstrahlung from the nuclear radiation drops sharply shortwards the Lyman limit; results are more dependent on the post-shock bremsstrahlung component which peaks in the soft X-rays (see fig. A3 in Contini et al. for illustrative examples). The choice of $n_{\rm o}$ imply densities downstream a factor of 10–100 higher, the higher for higher velocities, and thus within the range of those considered above.

Having selected the model parameters, we further assume that the estimated 1-keV emission comes from a region with the same size as that of the observed [Si VII] emission. Under those premises, the results are as follows. For NGC 1068, assuming that the free–free emission extends uniformly over a $\pi \times (70\,{\rm pc})^2$ cm^{-2} region (cf. Table 2), and models for shock velocities of 900 km s^{-1}, the inferred X-ray flux is larger by a factor of 20 compared with the nuclear 1-keV *Chandra* flux (Young et al. 2001). One may account for this difference by assuming a volume filling factor of 5–10 per cent, which in turn would account for the fact that free–free emission should mostly be produced locally at the shock front.

In Circinus we assume a free–free emission size of $\pi \times (30\,{\rm pc})^2$ cm^{-2} (cf. Table 1), and models of shock velocities of 500 km s^{-1}. In this case, the inferred X-ray flux is lower than the 1-keV *BeppoSAX* flux, as estimated in Prieto et al. (2004), by an order of magnitude. For the remaining two galaxies, we assume respective free–free emission areas (cf. Table 1) of 300 × 50 pc for ESO 428-G014 and $2 \times \pi\,(14\,{\rm pc})^2$ cm^{-2} for NGC 3081. Taking the models for shock velocities of 900 km s^{-1}, the inferred X-ray fluxes, when compared with 1-keV *BeppoSAX* fluxes (Maiolino et al. 1998), are of the same order for ESO 428-G014 and about an order of magnitude less in NGC 3081.

The above results are clearly dominated by the assumed size of the free–free emission region, which is unknown. The only purpose of this exercise is to show that under reasonable assumptions of shock velocities the shock associated free–free emission could be accommodated within the observed soft X-ray fluxes.

ACKNOWLEDGMENTS

Heino Falcke provided us with the 2-cm image of ESO 428-G014; Marcella Contini made a thorough review of the manuscript.

REFERENCES

Contini M., Viegas S., Prieto M. A., 2004, MNRAS, 348, 1065
Erkens U., Appenzeller I., Wagner S., 1997, A&A, 323, 707
Falcke H., Wilson A., Simpson C., 1998, ApJ, 502, 199
Ferguson J. W., Korista Kirk T., Ferland G., 1997, ApJS, 110, 287
Ferruit P., Wilson A., Mulchaey J., 2000, ApJS, 128, 139
Gallimore J., Baum S. A., O'Dea C. P., 2004, ApJ, 613, 794
Maiolino R. et al., 1998, A&A, 338, 781
Marco O., Alloin D., Beuzit J. L., 1997, A&A, 320, 399
Marconi A., Moorwood A. F. M., Salvati M., Oliva E., 1994, A&A, 291, 18
Moorwood et al., 1996, A&A, 315, L109
Nagar N., Wilson A., Mulchaey J., Gallimore J., 1999, ApJS, 120, 209
Oliva E. et al., 1994, A&A, 288, 457
Penston M. et al., 1984, MNRAS, 208, 347
Prieto M. A., Viegas S., 2000, ApJ, 532, 238
Prieto M. A. et al., 2004, ApJ, 614, 135
Reunanen J., Kotilainen J., Prieto M. A., 2003, MNRAS, 343, 192
Rodriguez-Ardila A. et al., 2004, in Ho C., Schmitt H., eds, Proc. IAU Symp. 222. Cambridge Univ. Press, Cambridge, p. 283
Veilleux S., Bland-Hawthorn J., 1997, ApJ, 479, L105
Weigelt G. et al., 2004, A&A, 425, 77
Wilson A. S., Baldwin J. A., 1989, AJ, 98, 2056
Wilson A. S. et al., 2000, ApJ, 120, 1325
Young A., Wilson A. S., Shopbell P. L., 2001, ApJ, 556, 23

This paper has been typeset from a TEX/LATEX file prepared by the author.